



Early Release Paper

## Heterozygosity for the Y701C *STAT1* mutation in a multiplex kindred with multifocal osteomyelitis

by Osamu Hirata, Satoshi Okada, Miyuki Tsumura, Reiko Kagawa, Mizuka Miki, Hiroshi Kawaguchi, Kazuhiro Nakamura, Stéphanie Boisson-Dupuis, Jean-Laurent Casanova, Yoshihiro Takihara, and Masao Kobayashi

*Haematologica* 2013 [Epub ahead of print]

Citation: Hirata O, Okada S, Tsumura M, Kagawa R, Miki M, Kawaguchi H, Nakamura K, Boisson-Dupuis S, Casanova JL, Takihara Y, and Kobayashi M. Heterozygosity for the Y701C *STAT1* mutation in a multiplex kindred with multifocal osteomyelitis. *Haematologica*. 2013; 98:xxx  
doi:10.3324/haematol.2013.083741

### *Publisher's Disclaimer.*

*E-publishing ahead of print is increasingly important for the rapid dissemination of science. Haematologica is, therefore, E-publishing PDF files of an early version of manuscripts that have completed a regular peer review and have been accepted for publication. E-publishing of this PDF file has been approved by the authors. After having E-published Ahead of Print, manuscripts will then undergo technical and English editing, typesetting, proof correction and be presented for the authors' final approval; the final version of the manuscript will then appear in print on a regular issue of the journal. All legal disclaimers that apply to the journal also pertain to this production process.*

Haematologica (pISSN: 0390-6078, eISSN: 1592-8721, NLM ID: 0417435, www.haematologica.org) publishes peer-reviewed papers across all areas of experimental and clinical hematology. The journal is owned by the Ferrata Storti Foundation, a non-profit organization, and serves the scientific community with strict adherence to the principles of open access publishing (www.doaj.org). In addition, the journal makes every paper published immediately available in PubMed Central (PMC), the US National Institutes of Health (NIH) free digital archive of biomedical and life sciences journal literature.

Support Haematologica and Open Access Publishing by becoming a member of the European Hematology Association (EHA) and enjoying the benefits of this membership, which include free participation in the online CME program

**Heterozygosity for the Y701C *STAT1* mutation  
in a multiplex kindred with multifocal osteomyelitis**

Osamu Hirata<sup>1</sup>, Satoshi Okada<sup>1, 2</sup>, Miyuki Tsumura<sup>1</sup>,  
Reiko Kagawa<sup>1</sup>, Mizuka Miki<sup>1</sup>, Hiroshi Kawaguchi<sup>1</sup>, Kazuhiro Nakamura<sup>1</sup>,  
Stéphanie Boisson-Dupuis<sup>2,3</sup>, Jean-Laurent Casanova<sup>2,3</sup>,  
Yoshihiro Takihara<sup>4</sup> and Masao Kobayashi<sup>1</sup>

**Author's affiliations**

<sup>1</sup>*Department of Pediatrics, Hiroshima University Graduate School of Biomedical & Health Sciences, Hiroshima, Japan*

<sup>2</sup>*St. Giles Laboratory of Human Genetics of Infectious Diseases, Rockefeller Branch, The Rockefeller University, New York, NY, USA*

<sup>3</sup>*Laboratory of Human Genetics of Infectious Diseases, Necker Branch, Inserm U980 and University Paris Descartes, Necker Medical School, Paris, France, EU*

<sup>4</sup>*Department of Stem Cell Biology, Research Institute for Radiation Biology and Medicine, Hiroshima University, Hiroshima, Japan*

**Statement of equal authors' contribution**

O.H. and S.O. contributed equally to this manuscript.

## **Running heads**

MSMD due to dominant negative mutation in STAT1

## **Contact information for correspondence**

Masao Kobayashi, M.D.

Department of Pediatrics, Hiroshima University Graduate School of Biomedical & Health Sciences, 1-2-3 Kasumi, Minami-ku, Hiroshima 734-8551, Japan.

Phone: +81-82-257-5212; Fax: +81-82-257-5214; E-mail: [masak@hiroshima-u.ac.jp](mailto:masak@hiroshima-u.ac.jp)

## **Word counts**

abstract 185 words, main text 3516 words, 1 table, 5 figures, 1 supplemental files (11 pages)

## **Acknowledgments**

The authors would like to thank Xiao-Fei Kong, MD, PhD, Vanessa Bryant, PhD, Dusan Bogunovic, PhD, Alexandra Kreins, MD, Marcela Moncada-Velez, BSc, Michael Ciancaneli, PhD, and Avinash Abhyankar, MD, PhD, for helpful discussions and critical reading. We also thank the members of the laboratory, Yelena Nemirovskaya and Eric Anderson for secretarial assistance, and Tiffany Nivare for technical assistance. Sequence analysis support was provided by the Analysis Center of Life Science, Natural Science Center for Basic Research and Development, Hiroshima University.

### **Grant support**

This study was supported, in part, by Grants in Aid for Scientific Research from the Japan Society for the Promotion of Science [22591161 to M.K.], and by Research on Measures for Intractable Diseases funding from the Japanese Ministry of Health, Labor and Welfare [H22-Nanchi-ippan-078 to M.K.]. This study was also supported, in part, by the Rockefeller University and grants from the National Center for Research Resources, and the National Center for Advancing Sciences (NCATS), National Institutes of Health (NIH) grant number 8UL1TR000043, NIH grant number R01AI089970, and the St. Giles Foundation. S.C. was supported by the AXA Research Fund and X-F.K. by the Stony Wold-Herbert Fund.

**Abstract**

Heterozygosity for dominant-negative *STAT1* mutations underlies autosomal dominant Mendelian susceptibility to mycobacterial diseases. Mutations conferring Mendelian susceptibility to mycobacterial diseases have been identified in the regions of the *STAT1* gene encoding the tail segment, DNA-binding domain and SH2 domain. We describe here a new heterozygous mutation, Y701C, in a Japanese two-generation multiplex kindred with autosomal dominant Mendelian susceptibility to mycobacterial diseases. This mutation affects precisely the canonical STAT1 tyrosine phosphorylation site. The Y701C STAT1 protein is produced normally, but its phosphorylation is abolished, resulting in a loss-of-function for STAT1-dependent cellular responses to IFN- $\gamma$  or IFN- $\alpha$ . In the patient's cells, the allele is dominant-negative for gamma-activated factor-mediated responses to IFN- $\gamma$ , but not for IFN-stimulated gene factor-3-mediated responses to IFN- $\alpha/\beta$ , accounting for the clinical phenotype of Mendelian susceptibility to mycobacterial diseases without severe viral diseases. Interestingly, both patients displayed multifocal osteomyelitis, which is often seen in Mendelian susceptibility to mycobacterial diseases patients with autosomal dominant partial IFN- $\gamma$ R1 deficiency. Multifocal osteomyelitis should thus prompt investigations of both STAT1 and IFN- $\gamma$ R1. This experiment of Nature also confirms the essential role of tyrosine 701 in human

STAT1 activity *in natura*.

## Introduction

Mendelian susceptibility to mycobacterial diseases (MSMD) (OMIM 209950) is a rare congenital disorder characterized by susceptibility to clinical disease caused by weakly virulent mycobacteria, such as *Mycobacterium bovis* Bacille Calmette-Guérin (BCG) and non tuberculous mycobacteria (NTM).<sup>1,2</sup> Affected individuals are also susceptible to *M. tuberculosis*, a more virulent mycobacterial species.<sup>3</sup> Nine MSMD-causing genes (*IFNGR1*, *IFNGR2*, *IL12B*, *IL12RB1*, *ISG15*, *STAT1*, *IRF8*, *CYBB* and *NEMO*) defining 17 different genetic etiologies have been identified to date.<sup>4-11</sup> Mutations of *IL12B*, *IL12RB1* and *NEMO* impair the production of IFN- $\gamma$ , whereas mutations of *IFNGR1*, *IFNGR2* and *STAT1* impair cellular responses to IFN- $\gamma$ . Moreover, autosomal recessive (AR) *ISG15* deficiency has recently been identified as a genetic cause of MSMD.<sup>11</sup> A lack of *ISG15* secretion by leukocytes results in impaired IFN- $\gamma$  production by NK and T lymphocytes, accounting for mycobacterial disease. Thus, single-gene variants disrupting IL-12- or *ISG15*-dependent, IFN- $\gamma$ -mediated immunity result in an inherited predisposition to mycobacterial infections.<sup>12,13</sup> However, no genetic etiology has yet been established for about half the patients with MSMD.

The first identification of MSMD-causing mutations of *STAT1* in 2001 was surprising, because *STAT1* is also involved in cellular responses mediated by cytokines

other than IFN- $\gamma$ , including IFN- $\alpha/\beta$  in particular. IFN- $\gamma$  stimulation results in the phosphorylation of STAT1 on tyrosine 701, inducing its homodimerization to form gamma-activated factor (GAF). GAF binds the gamma-activated sequence (GAS) to induce the transcription of target genes involved in antimycobacterial immunity. On the other hand, IFN- $\alpha/\beta$  stimulation induces the phosphorylation of both STAT1 and STAT2, resulting in the formation of the heterotrimeric IFN-stimulated gene factor-3 (ISGF3) complex with IRF9. ISGF3 recognizes IFN-stimulated response element (ISRE) motifs in target genes and their expression confers anti-viral immunity. Indeed, heterozygosity for *STAT1* dominant-negative alleles is responsible for AD MSMD.<sup>14-17</sup> Six mutations, E320Q, Q463H, K637E, M654K, K673R and L706S in *STAT1*, have been reported (Fig. 1A).<sup>14-17</sup> The L706S mutation affects the tail segment (TS) domain of STAT1, abolishing phosphorylation at Y701.<sup>14</sup> The E320Q and Q463H mutations affect the DNA-binding domain (DBD).<sup>15</sup> They have no effect on STAT1 phosphorylation, but modify the DNA-binding capacity of gamma-activated factor (GAF), impairing STAT1-dependent immunity. The other three mutations affect the SH2 domain. The M654K and K673R mutations impair the tyrosine phosphorylation of STAT1, whereas the K637E mutation impairs both STAT1 phosphorylation and GAF-DNA binding.<sup>16, 17</sup> These mutations are loss-of-function or hypomorphic and have been shown to exert a dominant-negative



effect on wild-type STAT1 for IFN- $\gamma$  responses.<sup>14, 15</sup> We report here the molecular and clinical features of a multiplex kindred with MSMD due to a new *STAT1* allele, with a mutation of the tyrosine 701 codon.

## **Methods**

### *Case report*

The patient (P1) is five-year-old Japanese boy born to a non consanguineous family (Fig. 1B). At the age of two months, he presented a mild fever and rash. Initial laboratory demonstrated leukocytosis (28,900/ $\mu$ l) with eosinophilia (11,100/ $\mu$ l) and a mild acute-phase inflammatory response. Treatment with cefotaxime was initiated and the patient's symptoms improved over the first two days, but leukocytosis with eosinophilia persisted for two weeks. No bacteria could be cultured from blood, pharynx and stool samples. P1 was vaccinated with BCG at the age of four months. At the age of three years, he suffered severe back pain and dysbasia. Laboratory tests revealed mild leukocytosis (13,900/ $\mu$ l) and high levels of C-reactive protein (3.99 mg/dl) and immunoglobulin (IgG; 2070 mg/dl) in the serum. Magnetic resonance imaging (MRI) and whole-body bone scintigraphy revealed multifocal osteomyelitis in three vertebrae and the cranial, costal, clavicular, bilateral tibial and pelvic bones. Histological findings

for the tibial bone were suggestive of a tuberculoid granulomas, but no pathogenic bacteria, including *Mycobacterium*, were detected in the tissues by PCR or culture. The leukocytes of the patient displayed a normal oxidative burst and normal proliferation in response to stimulation with PHA and ConA. *STAT1* sequencing revealed a heterozygous nucleotide substitution (2102 A>G) in exon 23, resulting in the substitution of a cysteine for a tyrosine residue at amino-acid position 701 (Y701C). P1 was started treatment with antimycobacterial drugs, including rifampicin (RFP), sulfamethoxazole/trimethoprim (ST) and clarithromycin (CAM). The clinical symptoms and laboratory findings have responded well to the treatment. These treatments have been maintained ever since, the patient now being five years old. The patient has had no episodes of severe viral infection. He has had mumps, chicken pox and flu, but all these diseases followed a normal clinical course. Normal levels of specific antibodies against these viruses were detected in P1 (Supplementary Table S1). At this time, he had not yet been vaccinated against measles and rubella.

His mother (P2) was vaccinated with BCG without complications in infancy. She had a history of multifocal osteomyelitis in the frontal bone, right maxilla, multiple vertebral bodies and ribs at 18 years of age. Initial laboratory tests showed a moderate acute-phase inflammatory response. Histological findings for the costal bone were

consistent with a granulomatous change. No pathogenic bacteria were detected. P2 was treated with levofloxacin hydrate (LVFX) and loxoprofen for two years. These treatments improved, but did not cure the symptoms. After this episode, P2 suffered from recurrent cervical and back pain. At the age of 38, confluent changes in the pressure on cervical and lumbar vertebrae were detected by on plain X ray, as a sequel of multifocal osteomyelitis. Since the identification of a heterozygous Y701C *STAT1* mutation in the family study, P2 has been treated with RFP, ST and CAM. This treatment appears to be effective, as the recurrent bone pain disappeared after treatment initiation. P2 presented no signs suggestive of immunodeficiency during childhood. She had no history of severe viral infection and normal levels of the specific antibodies against the Epstein–Barr, chicken pox, mumps, rubella and measles viruses (Supplementary Table S1).

We obtained blood samples from the patients, relatives, and healthy adult controls, after obtaining informed consent. This study was approved by the Ethics Committee/Internal Review Board of Hiroshima University.

The detailed methods of experiments are described in the Supplementary Methods section.

## Results

### *Identification of a new STAT1 mutation*

High-molecular weight genomic DNA was extracted from peripheral blood. The exons and the flanking introns of genes responsible for MSMD, including *STAT1*, *IFNGR1*, *IFNGR2*, *IL12B*, *IL12RB1* and *NEMO*, were amplified by PCR and analyzed by Sanger sequencing. We identified a new heterozygous mutation, 2102 A>G (Y701C), in exon 23 of *STAT1* in P1 (Fig. 1B). The Y701C mutation was not found in the National Center for Biotechnology Information, Ensembl or dbSNP databases, or in our own in-house database of 621 exomes. We also sequenced *STAT1* in 1,052 controls from 52 ethnic groups from the *Centre d'Etude du Polymorphisme Humain* and Human Genome Diversity panels; Y701C was not detected in these controls. This mutation was therefore considered to be a rare variant rather than an irrelevant polymorphism. Familial segregation analysis identified the same mutation in the subject's mother (P2), whereas the father and older brother were both wild-type and healthy. The mother had a history of multiple osteomyelitis of unknown etiology at 18 years of age, revealing an AD pattern of segregation of the MSMD clinical phenotype with heterozygosity for the *STAT1* allele. Figure 1A shows previously identified heterozygous or biallelic *STAT1*

mutations causing AD or AR genetic susceptibility to mycobacterial diseases.<sup>14-22</sup> The Y701C mutation affects the Y701 residue, the site of tyrosine phosphorylation in the STAT1 TS domain, a residue crucial for the activation of this molecule.<sup>23,24</sup>

*STAT1 phosphorylation and cytokine production by PBMCs in response to IFN- $\gamma$  stimulation*

IFN- $\gamma$ R1 is expressed ubiquitously, at moderate levels, on the cell surface, whereas very little IFN- $\gamma$ R2 is present and the expression of this receptor is tightly regulated, both spatially and temporally. Thus, IFN- $\gamma$ R2 is thought to be the factor determining responsiveness to IFN- $\gamma$ .<sup>25-27</sup> The CD14-positive monocytes in peripheral blood are known to express relatively high levels of IFN- $\gamma$ R2.<sup>28</sup> We therefore investigated the cellular response to IFN- $\gamma$ , focusing on CD14-positive monocytes. We purified CD14-positive monocytes by magnetic sorting and incubated them in the presence of LPS and various concentrations of IFN- $\gamma$ . We then collected the supernatant, in which we determined TNF levels. TNF production was severely impaired in the patients (P1 and P2), regardless of the dose of IFN- $\gamma$  used for stimulation (Fig. 1C). We analyzed STAT1 phosphorylation in response to IFN- $\gamma$  by flow cytometry. STAT1 phosphorylation levels were lower in CD14-positive monocytes from patients than in

control cells (Fig. 1D). The CD14-positive monocytes of both patients displayed severe impairment of TNF production in the presence of LPS and IFN- $\gamma$ , probably due to the impairment of Y701 phosphorylation in response to IFN- $\gamma$  stimulation.

#### *STAT1 phosphorylation and DNA-binding ability in EBV-B cells*

We assessed STAT1 production and phosphorylation in EBV-B cells from a healthy control (WT/WT), P1 (Y701C/WT), another patient with AD STAT1 deficiency (L706S/WT) and a patient with complete STAT1 deficiency (1760\_1761delAG/1760\_1761delAG, -/-), by immunoblotting (Fig. 2A).<sup>14, 20, 21</sup> STAT1 protein levels were normal in all EBV-B cells except those from a patient with complete STAT1 deficiency. However, STAT1 phosphorylation in response to IFNs stimulation was weak, but not abolished, in EBV-B cells carrying Y701C or L706S mutations. The DNA-binding ability of the mutant STAT1 proteins was analyzed by EMSA on EBV-B cells. EBV-B cells containing the Y701C or L706S STAT1 proteins displayed a partial impairment of GAF DNA-binding in response to stimulation with IFNs (Fig. 2C). The GAF-DNA binding complexes were shown, by supershift analysis, to consist of STAT1 homodimers, STAT3 homodimers and STAT1/3 heterodimers, following stimulation with IFN- $\gamma$  and IFN- $\alpha$ , respectively (data not shown). As previously described, GAF

was unable to bind DNA in response to IFN- $\gamma$  in EBV-B cells from a patients with complete STAT1 deficiency.<sup>20</sup> However, a complex identified as STAT3 homodimers was visible following incubation with IFN- $\alpha$ . By contrast, ISRE binding to DNA following IFN- $\alpha$  stimulation was found to be similar in cells from the patients and cells from controls, except for complete STAT1 deficiency. STAT1 phosphorylation and GAF DNA binding in EBV-B cells were impaired to a similar extent in P1 and P2 (Supplementary Fig. S1B, C). Overall, EBV-B cells from the patients displayed impaired, but not abolished, STAT1 phosphorylation in response to stimulation with IFNs, resulting in the partial impairment of GAF-DNA binding. However, ISRE-DNA binding levels in response to IFN- $\alpha$  stimulation were unaffected.

*The phosphorylation and nuclear translocation of Y701C STAT1 are impaired*

We transiently introduced WT and mutant *STAT1* into U3C cells by lipofection, and analyzed, by immunoblotting, the tyrosine 701 phosphorylation of the resulting protein in response to stimulation with IFN- $\alpha$  or IFN- $\gamma$  (Fig. 2B). Both Y701C and L706S *STAT1* proteins impaired phosphorylation. As previously reported, the phosphorylation of K673R *STAT1* was partially impaired.<sup>16</sup> By contrast, the Q463H *STAT1* mutant was phosphorylated to almost the same degree as the WT protein. We then analyzed the

nuclear translocation of STAT1 in U2OS cells stably expressing Flag-tagged WT, Q463H, K673R, L706S and Y701C STAT1 mutant alleles. Unphosphorylated STAT1 was mostly present in the cytoplasm before IFN- $\gamma$  stimulation (Supplementary Fig. S2A). After IFN- $\gamma$  stimulation, STAT1 was found in the nucleus in cells producing the WT and Q463H STAT1 proteins (Supplementary Fig. S2B). By contrast, STAT1 nuclear translocation was severely impaired in cells producing the Y701C and L706S STAT1 proteins. The K673R mutant STAT1 protein was present in both the nucleus and the cytoplasm, suggesting incomplete nuclear translocation. These results suggest that the Y701C mutation, like L706S, prevents STAT1 phosphorylation and nuclear translocation.

#### *Comparison of the Y701C and L706S mutations*

Both the Y701C and L706S mutations affect residues in the tail segment domain of STAT1. We focused on these two mutations and performed further functional characterization. We treated cells carrying these mutations with the tyrosine phosphatase inhibitor pervanadate and then analyzed the phosphorylation of STAT1 upon IFN- $\gamma$  stimulation.<sup>29</sup> STAT1 phosphorylation was restored in the presence of pervanadate in cells carrying the L706S mutation, whereas no such restoration was observed for the



Y701C mutant (Fig. 3A). Conversely, pervanadate treatment did not rescue GAF-DNA binding for L706S STAT1 (Fig. 3A). We investigated the mechanisms underlying these experimental observations, by extracting the cytosol and investigating STAT1 phosphorylation by immunoblotting (Fig. 3B). The L706S STAT1 protein displayed almost normal levels of phosphorylation in the cytosol fraction after pervanadate treatment, whereas phosphorylation was severely impaired in the nuclear fraction. These results suggest that the L706S mutation impairs both phosphorylation and nuclear translocation. Furthermore, this impairment of the nuclear translocation of L706S STAT1 was also confirmed by immunostaining (Fig. 3C). The L706S mutant protein was therefore considered to have at least two molecular defects: severe impairments of both the phosphorylation and nuclear translocation of STAT1. By contrast, Y701C STAT1 phosphorylation was totally abolished and could not be restored by pervanadate treatment.

#### *Transcriptional activity of the mutant STAT1 proteins*

We investigated the impact of the STAT1 Y701C mutation on the transcriptional activities of GAS and ISRE, by carrying out reporter assays with GAS or ISRE reporter plasmids. Production of the Y701C and L706S STAT1 proteins was associated with an

abolition of the transcriptional activities of both GAS and ISRE (Fig. 4A, C). Cotransfection experiments revealed that these mutant proteins had negative effects on the WT protein in GAS transcriptional activity (Fig. 4B). Furthermore, a dose-dependent negative-dominance effect was clearly observed for the Y701C and L706S mutant proteins. By contrast, ISRE transcriptional activity remained at almost normal levels in cells cotransfected with the L706S plasmid (Fig. 4C). The level of ISRE transcriptional activity was repeatedly found to be lower with Y701C STAT1, but no clear dominant negative effect was detected. These results are consistent with the results we observed in EMSA using EBV-B cells. Thus, the Y701C STAT1 allele has a dominant-negative effect, decreasing GAS activation but not ISRE activation.

#### *Downstream gene induction in CD14-positive monocytes and EBV-B cells*

The induction of downstream interferon-stimulated genes (ISGs) has been investigated with EBV-B cells from patients and in gene expression experiments using U3C cells.<sup>15</sup> We investigated the impact of the Y701C mutation further, by studying the induction of ISGs in CD14-positive monocytes from patients, comparing the results obtained with those for EBV-B cells. We first purified CD14-positive monocytes, stimulated them with IFN- $\gamma$  and analyzed the expression of the downstream ISGs encoding *CXCL9* and

*IRF1*, by RT-qPCR analysis. Strong induction of *CXCL9* was observed at late time points (6 hours) in healthy controls, but this induction was severely impaired in the patients' cells (Fig. 5A). In contrast, *IRF1* induction was observed at both early and late time points. The patients' cells displayed a mild but significant impairment of *IRF1* induction at late time points, whereas the difference observed at early time points is not significant. We then investigated the induction of *CXCL9*, *IRF1* and *ISG15* in EBV-B cells. The induction of these three ISGs was STAT1-dependent, as shown by the abolition of induction in STAT1-null EBV-B cells. EBV-B cells carrying heterozygous Y701C or L706S mutations displayed severely impaired induction of *CXCL9* and *ISG15* in response to IFNs (Fig. 5B, C). Unlike CD14-positive monocytes, the peak of *IRF1* induction was observed at early time points in EBV-B cells. The impairment of *IRF1* induction was mild and mostly observed at early time points in EBV-B cells from the patients. Thus, CD14-positive monocytes and EBV-B cells behaved similarly, but not identically, in terms of ISG induction in response IFN- $\gamma$  stimulation. These results suggest that the induction of ISGs is impaired in the patients' cells.

## **Discussion**

We report here a novel heterozygous *STAT1* mutation, 2102 A>G (Y701C), which results in STAT1 deficiency and AD MSMD. The Y701 residue serves as a site of phosphorylation for STAT1, this phosphorylation playing a key role in STAT1-mediated signal transduction. Indeed, AD *STAT1* mutations impairing STAT1 phosphorylation have been shown to underlie the pathogenesis of MSMD.<sup>14-17</sup> Furthermore, AD mutations that are gain-of-phosphorylation because they impair the nuclear dephosphorylation of STAT1 have been identified in patients with chronic mucocutaneous candidiasis.<sup>30-34</sup> The Y701C mutant STAT1 protein displayed a complete abolition of Y701 phosphorylation and downstream events, such as the nuclear translocation and transcriptional activities of GAS and ISRE. The Y701C *STAT1* allele is dominant for GAF, but recessive for ISGF3. This observation is highly consistent with previously identified STAT1 mutations in patients with AD STAT1 deficiencies and the molecular mechanisms can be explained by differences in the structure of GAS (homodimer of STAT1) and ISGF3 (heterodimer of STAT1/STAT2/IRF9).<sup>14-17</sup> The Y701C mutation is thus responsible for MSMD without viral disease. Two heterozygous *STAT1* mutations, Y701C and L706S, affect residues located in the same TS domain and result in the impairment of Y701 phosphorylation. However, these two mutants responded differently to stimulation in the presence of

pervanadate. This treatment rescued Y701 phosphorylation in L706S STAT1, but not in the Y701C protein. The functional defect seemed to be more severe for the Y701C than for the L706S mutant protein, as shown by GAS reporter assays and RT-qPCR analysis. The Y701C mutation may therefore have a stronger negative impact *in vitro* than L706S STAT1. However, by contrast to the findings of these *in vitro* studies, the clinical symptoms of the patient and his mother were similar to those of previously identified patients with AD STAT1 deficiency.

We also investigated the induction of ISGs upon IFN- $\gamma$  stimulation in CD14-positive monocytes from the patients. ISG induction has been intensively investigated in EBV-B cells<sup>15,17</sup>, but this is the first study to investigate the induction of ISGs in primary cells from patients. Both EBV-B cell lines and primary monocytes from the patients displayed a severe impairment of *CXCL9* induction. Minor differences in induction patterns were observed, but both types of cell displayed a mild impairment of *IRF1* induction. Thus, the impairment of ISG induction was confirmed not only in EBV-B cells, but also in the patients' monocytes. IL-12p40 induction is totally dependent on *Irf1* in mice.<sup>35-37</sup> Macrophages from *Irf1*-null mice display impaired induction of inducible nitric oxide synthase (iNOS) in response to lipopolysaccharide.<sup>38</sup>

<sup>39</sup> Furthermore, *Irf1*-null mice develop severe symptoms when infected with

*Mycobacterium bovis*. Thus, the impairment of *IRF1* induction observed in CD14-positive monocytes may contribute to host susceptibility to mycobacteria. We also observed an impairment in *ISG15* induction in the patients' EBV-B cells. The recent identification of ISG15 deficiency in some human patients with MSMD has provided evidence of an important role for this molecule in host immunity to mycobacteria.<sup>11</sup> Heterozygous *STAT1* mutations thus have negative effects on the downstream induction of ISGs involved in host defense against mycobacteria, and this *in vitro* cellular phenotype is commonly observed in the patients' cells. However, the magnitude of this negative impact may differ between cell types and between the ISGs induced. The induction of ISGs is also intensively investigated in patients with AR *STAT1* deficiency.<sup>22</sup> Similar to the current study, the severity of impairments was differently observed in the patient's cells depending on the ISGs induced. These observations reflect the complexity of *STAT1*-mediated signaling.<sup>40</sup>

Including the two patients studied here, 11 patients with AD *STAT1* deficiency have been identified to date. Five of these 11 patients have developed multifocal osteomyelitis, a typical clinical feature of patients with AD partial *IFN-γR1* deficiency.<sup>4,</sup>

<sup>41</sup> Our initial patient showed multifocal osteomyelitis showing tuberculoid granulomas without the detection of pathogenic mycobacterium by culture and/or PCR

amplification. Additionally, his mother had a history of multifocal osteomyelitis. Thus, these observations emphasize the importance of multifocal osteomyelitis as one of the representative clinical manifestation even in patients with AD STAT1 deficiency. We summarized the clinical manifestations of 11 patients with AD STAT1 deficiency<sup>14-17</sup>, 53 patients with AD partial IFN- $\gamma$ R1 deficiency<sup>41-45</sup>, 14 patients with AR partial IFN- $\gamma$ R1 deficiency<sup>46</sup> and 102 patients with AR IL-12R $\beta$ 1 deficiency<sup>47</sup>, the most common genetic etiology of MSMD (Table 1). Multifocal osteomyelitis had a high frequency in AD STAT1 deficiency (45.5%), AD partial IFN- $\gamma$ R1 deficiency (79.2%) and AR partial IFN- $\gamma$ R1 deficiency (50.0%), but was less frequent in patients with AR complete IFN- $\gamma$ R1 deficiency (13%).<sup>41</sup> Unfortunately, this clinical manifestation has not been investigated in patients with AR IL-12R $\beta$ 1 deficiency.<sup>47</sup> In many cases, either BCG or environmental mycobacteria have been proved by biopsy of osteomyelitis. By contrast, the frequency of BCG disease, a common sign in patients with MSMD, in patients vaccinated with BCG is similar AD STAT1 deficiency (77.8%), AD partial IFN- $\gamma$ R1 deficiency (76.7%), AR partial IFN- $\gamma$ R1 deficiency (85.7 %) and AR IL-12R $\beta$ 1 deficiency (77.9%). The clinical signs of AD STAT1 deficiency may therefore be considered to be similar to those of partial IFN- $\gamma$ R1 deficiency. There are several possible reasons for this: i) STAT1 is a non redundant downstream transcription factor

for IFN- $\gamma$  signaling<sup>4</sup>, ii) STAT1 mutations impair GAF-mediated signaling, but not ISGF3-mediated signaling, and IFN- $\gamma$  induces GAF, but not ISGF3<sup>48</sup>, iii) IFN- $\gamma$  signaling is only partially impaired in both disorders.<sup>4</sup> The clinical similarities between these two disorders support our hypothesis that the symptoms accompanying AD STAT1 deficiency result from an impairment of cellular responses to IFN- $\gamma$ . Multifocal osteomyelitis is a characteristic symptom common to three different disorders: AD partial IFN- $\gamma$ R1 deficiency, AR partial IFN- $\gamma$ R1 deficiency and AD STAT1 deficiency. Multifocal osteomyelitis should therefore lead to investigations of both STAT1 and IFN- $\gamma$ R1.



### **Authorship and Disclosures**

O.H and S.O. contributed equally to this manuscript. Correspondence should be addressed to Masao Kobayashi. O.H, S.O and M.T. were involved in research design, experiments and data analysis; O.H and S.O. wrote the manuscript; R.K, M.M, H.K and K.N. treated the patients; S.B.-D., J.-L.C., Y.T. and M.K. directed experiments and edited the paper; S.B.-D, J.-L.C., Y.T. and M.K. supervised all work. The authors declare that they have no conflict of interest.

## References

1. Casanova JL, Abel L. Genetic dissection of immunity to mycobacteria: the human model. *Annu Rev Immunol.* 2002;20:581-620.
2. Hamosh A, Scott AF, Amberger JS, Bocchini CA, McKusick VA. Online Mendelian Inheritance in Man (OMIM), a knowledgebase of human genes and genetic disorders. *Nucleic Acids Res.* 2005;33(Database issue):D514-7.
3. Alcais A, Fieschi C, Abel L, Casanova JL. Tuberculosis in children and adults: two distinct genetic diseases. *The Journal of experimental medicine.* 2005;202(12):1617-21.
4. Filipe-Santos O, Bustamante J, Chagnier A, Vogt G, de Beaucoudrey L, Feinberg J, et al. Inborn errors of IL-12/23- and IFN-gamma-mediated immunity: molecular, cellular, and clinical features. *Semin Immunol.* 2006;18(6):347-61.
5. Vogt G, Bustamante J, Chagnier A, Feinberg J, Boisson Dupuis S, Picard C, et al. Complementation of a pathogenic IFNGR2 misfolding mutation with modifiers of N-glycosylation. *J Exp Med.* 2008;205(8):1729-37.
6. Bustamante J, Arias AA, Vogt G, Picard C, Galicia LB, Prando C, et al. Germline CYBB mutations that selectively affect macrophages in kindreds with X-linked predisposition to tuberculous mycobacterial disease. *Nat Immunol.* 2011;12(3):213-21.
7. Hambleton S, Salem S, Bustamante J, Bigley V, Boisson-Dupuis S, Azevedo J, et al. IRF8 mutations and human dendritic-cell immunodeficiency. *The New England journal of medicine.* 2011;365(2):127-38.
8. Al-Muhsen S, Casanova JL. The genetic heterogeneity of mendelian susceptibility to mycobacterial diseases. *J Allergy Clin Immunol.* 2008;122(6):1043-51; quiz 52-3.
9. Boisson-Dupuis S, Kong XF, Okada S, Cypowyj S, Puel A, Abel L, et al. Inborn errors of human STAT1: allelic heterogeneity governs the diversity of immunological and infectious phenotypes. *Current opinion in immunology.* 2012;24(4):364-78.
10. Casanova JL, Holland SM, Notarangelo LD. Inborn errors of human JAKs and STATs. *Immunity.* 2012;36(4):515-28.
11. Bogunovic D, Byun M, Durfee LA, Abhyankar A, Sanal O, Mansouri D, et al. Mycobacterial Disease and Impaired IFN-gamma Immunity in Humans with Inherited ISG15 Deficiency. *Science.* 2012;337(6102):1684-8.
12. Casanova JL, Abel L. Inborn errors of immunity to infection: the rule rather than the exception. *The Journal of experimental medicine.* 2005;202(2):197-201.
13. Alcais A, Quintana-Murci L, Thaler DS, Schurr E, Abel L, Casanova JL. Life-threatening infectious diseases of childhood: single-gene inborn errors of immunity? *Ann N Y Acad Sci.* 2010;1214:18-33.

14. Dupuis S, Dargemont C, Fieschi C, Thomassin N, Rosenzweig S, Harris J, et al. Impairment of mycobacterial but not viral immunity by a germline human STAT1 mutation. *Science*. 2001;293(5528):300-3.
15. Chapgier A, Boisson-Dupuis S, Jouanguy E, Vogt G, Feinberg J, Prochnicka-Chalufour A, et al. Novel STAT1 alleles in otherwise healthy patients with mycobacterial disease. *PLoS Genet*. 2006;2(8):e131.
16. Tsumura M, Okada S, Sakai H, Yasunaga S, Ohtsubo M, Murata T, et al. Dominant-negative STAT1 SH2 domain mutations in unrelated patients with Mendelian susceptibility to mycobacterial disease. *Human mutation*. 2012;33(9):1377-87.
17. Sampaio EP, Bax HI, Hsu AP, Kristosturyan E, Pechacek J, Chandrasekaran P, et al. A Novel STAT1 Mutation Associated with Disseminated Mycobacterial Disease. *Journal of clinical immunology*. 2012; 32(4):681-9.
18. Kristensen IA, Veirum JE, Moller BK, Christiansen M. Novel STAT1 Alleles in a Patient with Impaired Resistance to Mycobacteria. *Journal of clinical immunology*. 2011;31(2):265-71.
19. Vairo D, Tassone L, Tabellini G, Tamassia N, Gasperini S, Bazzoni F, et al. Severe impairment of IFN-gamma and IFN-alpha responses in cells of a patient with a novel STAT1 splicing mutation. *Blood*. 2011;118(7):1806-17.
20. Dupuis S, Jouanguy E, Al-Hajjar S, Fieschi C, Al-Mohsen IZ, Al-Jumaah S, et al. Impaired response to interferon-alpha/beta and lethal viral disease in human STAT1 deficiency. *Nat Genet*. 2003;33(3):388-91.
21. Chapgier A, Wynn RF, Jouanguy E, Filipe-Santos O, Zhang S, Feinberg J, et al. Human complete Stat-1 deficiency is associated with defective type I and II IFN responses in vitro but immunity to some low virulence viruses in vivo. *J Immunol*. 2006;176(8):5078-83.
22. Kong XF, Ciancanelli M, Al-Hajjar S, Alsina L, Zumwalt T, Bustamante J, et al. A novel form of human STAT1 deficiency impairing early but not late responses to interferons. *Blood*. 2010;116(26):5895-906.
23. Shuai K, Ziemiecki A, Wilks AF, Harpur AG, Sadowski HB, Gilman MZ, et al. Polypeptide signalling to the nucleus through tyrosine phosphorylation of Jak and Stat proteins. *Nature*. 1993;366(6455):580-3.
24. Chen X, Vinkemeier U, Zhao Y, Jeruzalmi D, Darnell JE, Jr., Kuriyan J. Crystal structure of a tyrosine phosphorylated STAT1 dimer bound to DNA. *Cell*. 1998;93(5):827-39.
25. Bach EA, Aguet M, Schreiber RD. The IFN gamma receptor: a paradigm for cytokine receptor signaling. *Annual review of immunology*. 1997;15:563-91.
26. van Boxel-Dezaire AH, Stark GR. Cell type-specific signaling in response to interferon-gamma. *Curr Top Microbiol Immunol*. 2007;316:119-54.

27. Kong XF, Vogt G, Itan Y, Macura-Biegun A, Szafarska A, Kowalczyk D, et al. Haploinsufficiency at the human IFNGR2 locus contributes to mycobacterial disease. *Human molecular genetics*. 2012.
28. Bernabei P, Coccia EM, Rigamonti L, Bosticardo M, Forni G, Pestka S, et al. Interferon-gamma receptor 2 expression as the deciding factor in human T, B, and myeloid cell proliferation or death. *J Leukoc Biol*. 2001;70(6):950-60.
29. Tourkine N, Schindler C, Larose M, Houdebine LM. Activation of STAT factors by prolactin, interferon-gamma, growth hormones, and a tyrosine phosphatase inhibitor in rabbit primary mammary epithelial cells. *The Journal of biological chemistry*. 1995;270(36):20952-61.
30. Liu L, Okada S, Kong XF, Kreins AY, Cypowyj S, Abhyankar A, et al. Gain-of-function human STAT1 mutations impair IL-17 immunity and underlie chronic mucocutaneous candidiasis. *The Journal of experimental medicine*. 2011;208(8):1635-48.
31. van de Veerdonk FL, Plantinga TS, Hoischen A, Smeekens SP, Joosten LA, Gilissen C, et al. STAT1 mutations in autosomal dominant chronic mucocutaneous candidiasis. *The New England journal of medicine*. 2011;365(1):54-61.
32. Smeekens SP, Plantinga TS, van de Veerdonk FL, Heinhuis B, Hoischen A, Joosten LA, et al. STAT1 Hyperphosphorylation and Defective IL12R/IL23R Signaling Underlie Defective Immunity in Autosomal Dominant Chronic Mucocutaneous Candidiasis. *PLoS One*. 2011;6(12):e29248.
33. Takezaki S, Yamada M, Kato M, Park MJ, Maruyama K, Yamazaki Y, et al. Chronic Mucocutaneous Candidiasis Caused by a Gain-of-Function Mutation in the STAT1 DNA-Binding Domain. *Journal of immunology*. 2012;189(3):1521-6.
34. Toth B, Mehes L, Tasko S, Szalai Z, Tulassay Z, Cypowyj S, et al. Herpes in STAT1 gain-of-function mutation [corrected]. *Lancet*. 2012;379(9835):2500.
35. Taniguchi T, Ogasawara K, Takaoka A, Tanaka N. IRF family of transcription factors as regulators of host defense. *Annu Rev Immunol*. 2001;19:623-55.
36. Taki S, Sato T, Ogasawara K, Fukuda T, Sato M, Hida S, et al. Multistage regulation of Th1-type immune responses by the transcription factor IRF-1. *Immunity*. 1997;6(6):673-9.
37. Lohoff M, Ferrick D, Mittrucker HW, Duncan GS, Bischof S, Rollinghoff M, et al. Interferon regulatory factor-1 is required for a T helper 1 immune response in vivo. *Immunity*. 1997;6(6):681-9.
38. Kamijo R, Harada H, Matsuyama T, Bosland M, Gerecitano J, Shapiro D, et al. Requirement for transcription factor IRF-1 in NO synthase induction in macrophages. *Science*. 1994;263(5153):1612-5.

39. Martin E, Nathan C, Xie QW. Role of interferon regulatory factor 1 in induction of nitric oxide synthase. *The Journal of experimental medicine*. 1994;180(3):977-84.
40. Gough DJ, Levy DE, Johnstone RW, Clarke CJ. IFN $\gamma$  signaling: does it mean JAK-STAT? *Cytokine & growth factor reviews*. 2008;19(5-6):383-94.
41. Dorman SE, Picard C, Lammas D, Heyne K, van Dissel JT, Baretto R, et al. Clinical features of dominant and recessive interferon gamma receptor 1 deficiencies. *Lancet*. 2004;364(9451):2113-21.
42. Hoshina T, Takada H, Sasaki-Mihara Y, Kusuhara K, Ohshima K, Okada S, et al. Clinical and Host Genetic Characteristics of Mendelian Susceptibility to Mycobacterial Diseases in Japan. *Journal of clinical immunology*. 2011;31(3):309-14.
43. Lee WI, Huang JL, Lin TY, Hsueh C, Wong AM, Hsieh MY, et al. Chinese patients with defective IL-12/23-interferon-gamma circuit in Taiwan: partial dominant interferon-gamma receptor 1 mutation presenting as cutaneous granuloma and IL-12 receptor beta1 mutation as pneumatocele. *Journal of clinical immunology*. 2009;29(2):238-45.
44. Glosli H, Stray-Pedersen A, Brun AC, Holtmon LW, Tonjum T, Chapgier A, et al. Infections due to various atypical mycobacteria in a Norwegian multiplex family with dominant interferon-gamma receptor deficiency. *Clin Infect Dis*. 2008;46(3):e23-7.
45. Okada S, Ishikawa N, Shirao K, Kawaguchi H, Tsumura M, Ohno Y, et al. The novel IFNGR1 mutation 774del4 produces a truncated form of interferon-gamma receptor 1 and has a dominant-negative effect on interferon-gamma signal transduction. *J Med Genet*. 2007;44(8):485-91.
46. Sologuren I, Boisson-Dupuis S, Pestano J, Vincent QB, Fernandez-Perez L, Chapgier A, et al. Partial recessive IFN- $\gamma$ R1 deficiency: genetic, immunological and clinical features of 14 patients from 11 kindreds. *Hum Mol Genet*. 2011;20(8):1509-23.
47. de Beaucoudrey L, Samarina A, Bustamante J, Cobat A, Boisson-Dupuis S, Feinberg J, et al. Revisiting Human IL-12Rbeta1 Deficiency: A Survey of 141 Patients From 30 Countries. *Medicine (Baltimore)*. 2010;89(6):381-402.
48. Ginter T, Bier C, Knauer SK, Sughra K, Hildebrand D, Munz T, et al. Histone deacetylase inhibitors block IFN $\gamma$ -induced STAT1 phosphorylation. *Cellular signalling*. 2012;24(7):1453-60.

**Table 1** Comparison of clinical manifestations

	AD	STAT1	AD	partial	AR	partial	AR	IL-12R $\beta$ 1
		deficiency	IFN- $\gamma$ R1		IFN- $\gamma$ R1		deficiency	
			deficiency		deficiency		Reference	
No. of cases	11		53		14		102	
onset of MSMD	5.3y		10.8y		11.2y		2.4y (0.1y-31y)	
	(0.5y-18y)		(0.1y-62y)		(0.1y-31y)			
BCG disease	7/9		23/30		6/7		67/86	
(among vaccinated patients)								
Environmental mycobacteria	5/11		42/53		6/14		19/102	
<i>M. tuberculosis</i> complex			2/53		1/14		5/102	
<i>Salmonella</i> spp	none		2/53		3/14		44/102	
Severe infection	viral none		1/53		none		none	

Osteomyelitis	5/11	42/53	7/14	
Locations of mycobacterial infections				
Nodes	2/11	30/53		6/14
Other organs	4/11	11/53		6/14
References	14-17	41-45	46	47

---

## Legends to Figures

### Figure 1.

(A) Summary of loss-of-function *STAT1* mutations. The N-terminal domain, coiled-coil domain, DNA-binding domain, linker domain, SH2 domain, tail segment domain (TS), and transactivation domain (TA) are shown, together with Y701, the site of tyrosine phosphorylation. The dominant-negative mutants (blue) are indicated below the protein and the recessive forms of hypomorphic (green) and loss-of-function mutations (yellow) are shown above the protein. Y701C is shown in red. (B) The heterozygous Y701C mutation was detected in the patient (II.2) and his mother (I.2). Closed symbols indicate the affected individual and open symbols indicate a healthy family member. (C) CD14-positive monocytes were incubated in the presence of LPS (100 ng/ml) and various concentrations of IFN- $\gamma$  for 48 hours and TNF production was then analyzed. CD14-positive monocytes from the patient (P1 and P2) produced abnormally small amounts of TNF. Two independent experiments were performed. (D) Flow cytometry analysis of STAT1 phosphorylation upon IFN- $\gamma$  stimulation, on peripheral monocytes (CD14<sup>+</sup> gate). STAT1 phosphorylation levels were lower in the patients' cells than in control cells. The black line indicates an absence of stimulation and the red line, stimulation with 10<sup>4</sup> IU/ml IFN- $\gamma$ . Three independent experiments were performed.



**Figure 2. STAT1 phosphorylation and DNA-binding ability in EBV-B cells**

STAT1 production and phosphorylation in EBV-B cells (A) and transiently transfected U3C cells (B). The cells were stimulated with  $10^5$  IU/ml IFN for 15 min and subjected to immunoblot analysis. (A) EBV-B cells carrying heterozygous Y701C or L706S mutations showed a marked impairment of phosphorylation. The level of pSTAT1 was decreased in Y701C or L706S carrying cells up to 50.0 % or 57.6 % after IFN- $\gamma$  stimulation and up to 66.3 % or 61.5 % after IFN- $\alpha$  stimulation when they are compared with healthy control, respectively. (B) The Q463H STAT1 protein was normally phosphorylated, to levels similar to those observed for the WT protein. K673R STAT1 was only weakly phosphorylated. The Y701C STAT1 protein was not phosphorylated. (C) DNA-binding ability in EBV-B cells, as assessed by EMSA with GAS and ISRE probes. EBV-B cells carrying Y701C or L706S mutations displayed a marked impairment of GAS DNA-binding ability. This impairment was particularly strong after IFN- $\gamma$  stimulation. The ability of ISGF3 to bind DNA upon stimulation with IFN- $\alpha$  was preserved at almost normal levels in the patients' cells. At least two independent experiments were performed. (G:  $10^5$  IU/ml IFN- $\gamma$ , A:  $10^5$  IU/ml IFN- $\alpha$ )

**Figure 3. Comparison of the Y701C and L706S mutations**

(A) U3C transfectants were stimulated with  $10^5$  IU/ml IFN- $\gamma$  in the presence or absence of pervanadate for 15 min and subjected to immunoblotting and EMSA. The L706S STAT1 protein was phosphorylated to almost normal levels in response to IFN- $\gamma$  stimulation in the presence of pervanadate, whereas no phosphorylation of the Y701C STAT1 protein was observed. However, L706S STAT1 was still associated with a lack of GAF-DNA binding, even after its phosphorylation had been restored. (B) STAT1 phosphorylation was investigated in the nuclear and cytosolic fractions, by immunoblotting. The phosphorylated L706S STAT1 protein was mostly present in the cytosol fraction. (C) U2OS cells stably expressing Flag-tagged WT, Y701C, or L706S STAT1 were stimulated with IFN- $\gamma$  for 30 min in the presence or absence of pervanadate and subjected to immunostaining. Nuclear translocation was severely impaired in cells producing either Y701C or L706S STAT1, even after pervanadate treatment. At least two independent experiments were carried out.

**Figure 4. Effect of *STAT1* mutation on transcriptional activity**

U3C cells were transiently cotransfected with plasmids carrying the WT and/or mutant *STAT1* and with GAS (A, B) or ISRE (C, D) reporter plasmids. The quantities of the

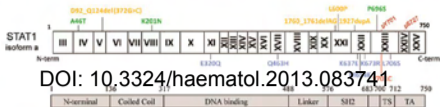
plasmids used are indicated under the bar. The cells were stimulated with IFN- $\gamma$  (for 16 hours) or IFN- $\alpha$  (for 12 hours), 24 hours after transfection. (A) The Y701C and L706S *STAT1* mutations abolished GAS transcriptional activity. Cotransfection experiments revealed that cells producing mutant STAT1 proteins had just under a quarter the GAS transcriptional activity of cells producing the WT protein. (B) A dose-dependent negative effect on WT protein activity was observed in cells cotransfected with Y701C and L706S constructs. (C, D) The Y701C and L706S *STAT1* mutations abolished ISRE transcriptional activity. A negative effect was suspected in cells cotransfected with the Y701C construct, but no clear dominant-negative effects on ISRE transcriptional activity were demonstrated. The error bars indicate the SD of one experiment carried out in triplicate. At least two independent experiments were performed.

### **Figure 5. Analysis of gene expression**

The induction of ISGs was analyzed by RT-qPCR. (A) CD14-positive monocytes from the patient (P1, P2) and two healthy controls were stimulated with  $10^3$  IU/ml IFN- $\gamma$  (for 2 or 6 hours) and the induction of *CXCL9* and *IRF1* was investigated. The induction of *CXCL9* was severely impaired in the patients' cells, whereas the induction of *IRF1* was only mildly impaired. \*Differences were statistically significant in monocytes from the

patient compared with those from healthy individuals ( $P < 0.05$ ). (B, C) The induction of *CXCL9*, *IRF1* and *ISG15* in EBV-B cells from the patients, Y701C/WT and L706S/WT cells, and cells from healthy individuals, in response to IFN- $\gamma$  (B) or IFN- $\alpha$  (C) stimulation. EBV-B cells carrying Y701C or L706S mutations displayed a severe impairment of *CXCL9* induction in response to IFN stimulation. The induction of *IRF1* and *ISG15* was also impaired, but was milder than that of *CXCL9*. ISG expression was normalized with respect to *GAPDH*. The results shown are representative of three independent experiments, except for the CD14<sup>+</sup> monocyte experiment (which was performed twice). Differences were statistically significant in the cells carrying the Y701C mutation \*( $p < 0.05$ ) or L706S mutation †( $p < 0.05$ ) compared with EBV-B cells from healthy individuals.

Figure 1A



DOI: 10.3324/haematol.2013.083741

Figure 1B

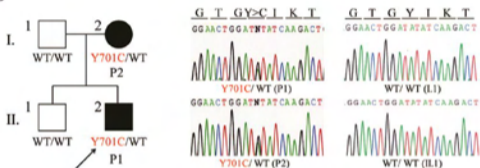


Figure 1C

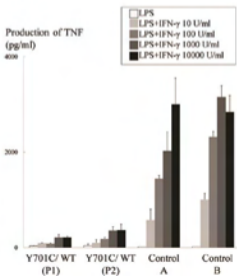
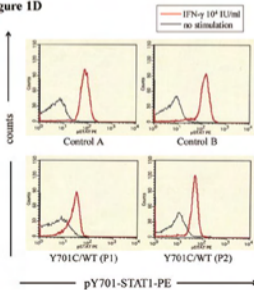


Figure 1D



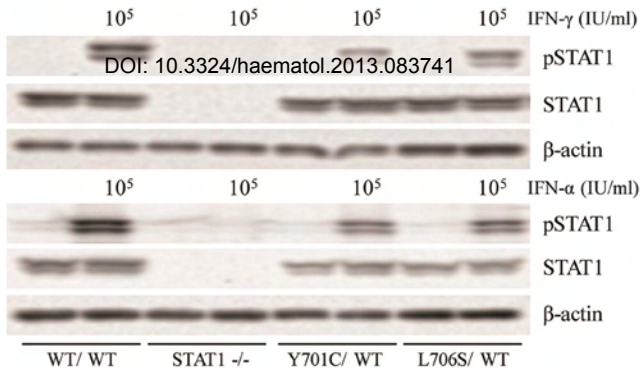
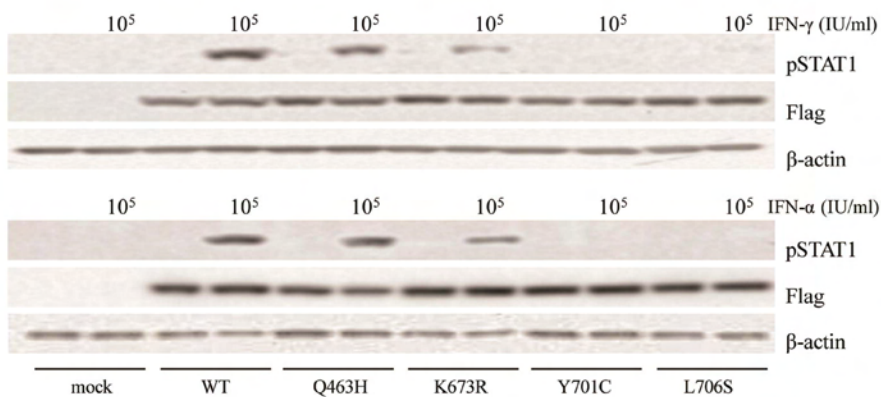
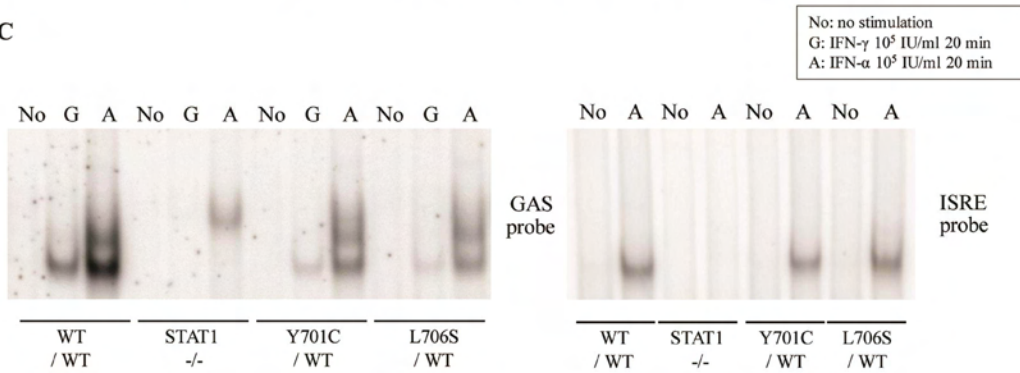
**Figure 2A****Figure 2B****Figure 2C**

Figure 3A

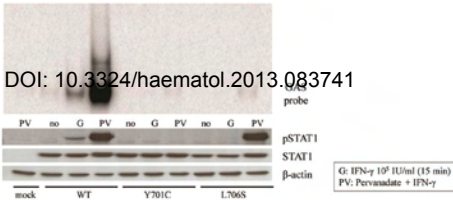


Figure 3B

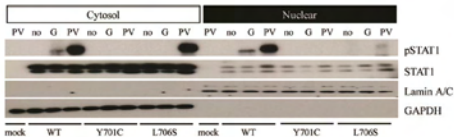
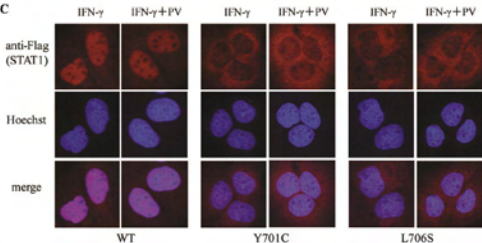
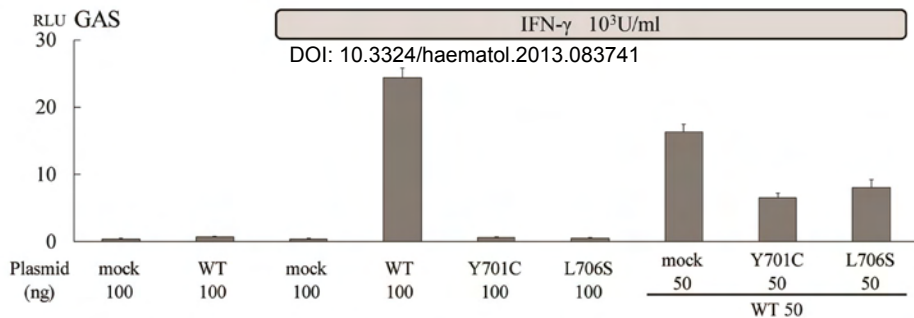
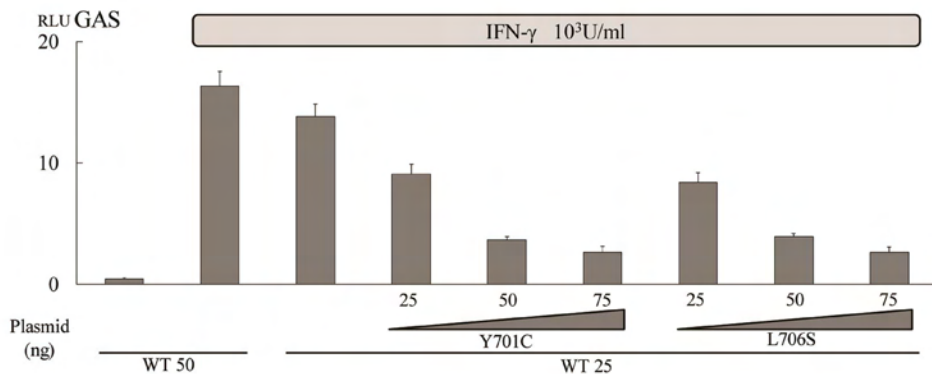
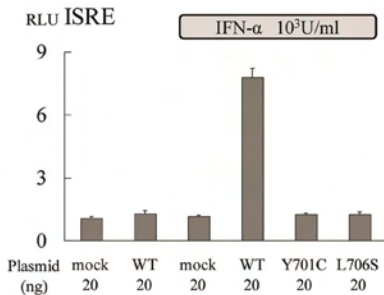
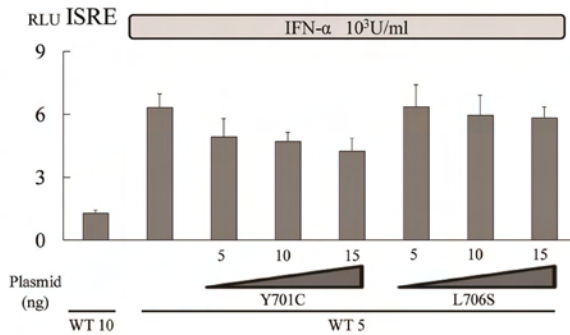
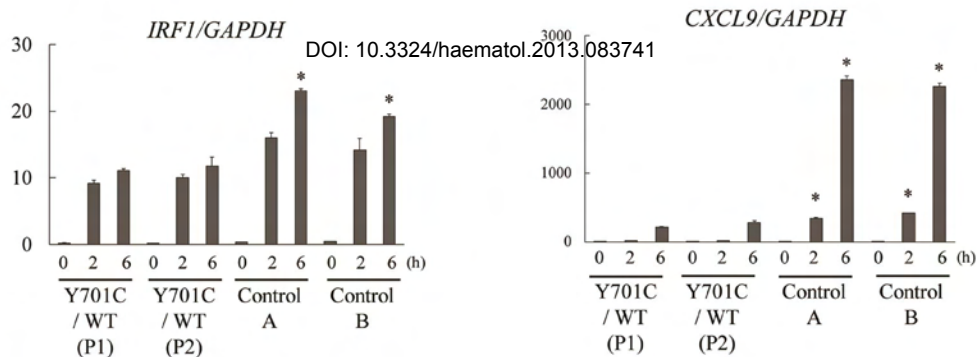
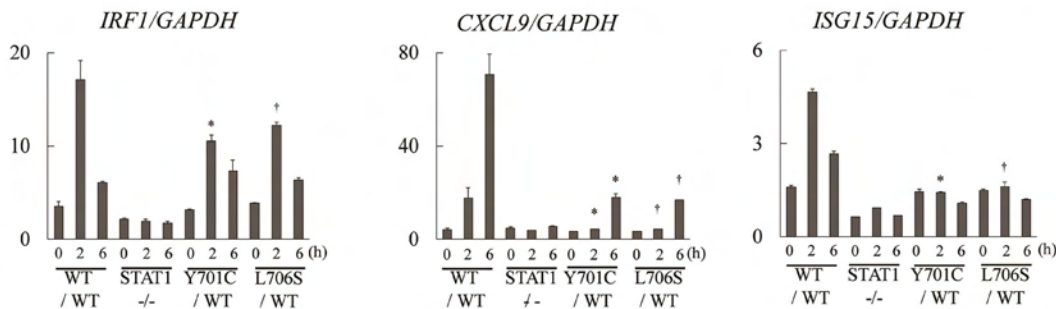
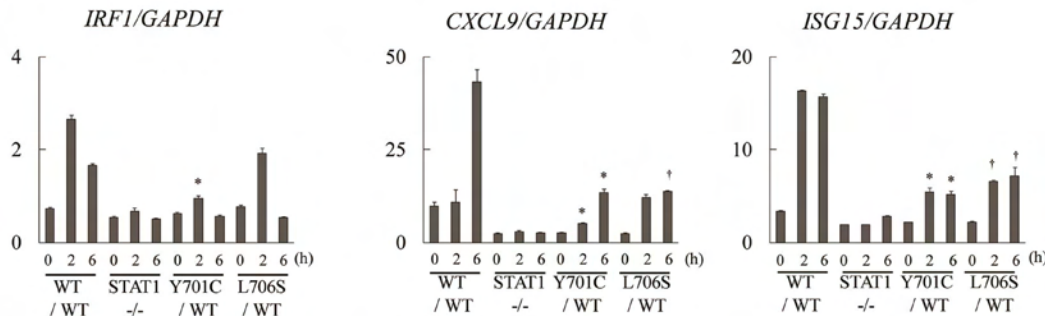


Figure 3C



**Figure 4A****Figure 4B****Figure 4C****Figure 4D**



**Figure 5A** : IFN- $\gamma$   $10^3$  IU/ml**Figure 5B** : IFN- $\gamma$   $10^3$  IU/ml**Figure 5C** : IFN- $\alpha$   $10^3$  IU/ml

## Supplementary methods

### *Molecular genetic analysis*

*STAT1* and its flanking introns were amplified by PCR and sequenced. Total RNA was extracted from peripheral blood mononuclear cells (PBMCs) with ISOGEN (NIPPON GENE CO, Japan), and complementary DNA (cDNA) was synthesized by reverse transcription. The wild-type (WT) and Y701C mutant alleles were amplified by PCR, spanning the entire coding region of *STAT1*. The PCR products were inserted into the pGEM-T Easy vector (Promega, USA) and their sequences were confirmed. We generated constructs encoding the L706S, Q463H, and K673R mutant forms of STAT1, by performing PCR-based mutagenesis of the WT construct with mismatched PCR primers. The resulting fragments were inserted, in frame, between the *Bam*HI and *Eco*RV sites of the pcDNA-C-Flag mammalian expression vector. Primer sequences and PCR conditions are available on request.

### *Analysis of gene expression*

Epstein-Barr virus-transformed B (EBV-B) cells from control individuals, the patient from Kindred A and patients carrying L706S *STAT1* mutations were maintained in RPMI1640 supplemented with 20% fetal bovine serum (FBS) (Thermo Scientific, USA).

U3C STAT1-null fibrosarcoma cells were maintained in DMEM supplemented with 10% FBS. The plasmids carrying the WT and each of the mutant STAT1 genes were transferred, individually, into U3C cells by lipofection (Invitrogen, USA). EBV-B cells and transfected U3C cells were left unstimulated or were stimulated with  $10^5$  IU/ml of IFNs for 15 minutes and subjected to immunoblot analysis. Pervanadate was prepared by mixing orthovanadate with  $H_2O_2$  and incubating for 15 minutes at  $22^\circ C$ . U3C transfectants were treated with pervanadate (0.8 mM orthovanadate mixed with 0.2 mM  $H_2O_2$ ) for five minutes before stimulation with IFN- $\gamma$ . We investigated the nuclear and cytoplasmic fractions, by stimulating U3C transfectants with IFN- $\gamma$  and then isolating these fractions with NE-PER Nuclear and Cytoplasmic Extraction Regents (Thermo Scientific), according to the manufacturer's protocol. Information about the antibodies used is provided in Supplementary Table S2.

### *Immunostaining*

U2OS human bone osteosarcoma epithelial cells stably expressing a Flag-tagged WT or mutant STAT1 construct were generated by lipofection and selected on 1 mg/ml G418 (Calbiochem, Germany). Immunostaining was carried out as previously described (16). Images were acquired with a BZ-8000 fluorescence microscope (KEYENCE, Japan).

All immunostaining images were obtained with identical exposure times, to optimize comparison.

#### *Luciferase reporter assay*

Reporter plasmids (Cignal™ GAS or ISRE Reporter Assay Kit; SABiosciences, Germany) and WT and/or mutant STAT1-encoding plasmids were transferred into U3C cells by lipofection. Six hours after transfection, the cells were transferred to a medium containing 1% FBS, in which they were cultured for 18 hours. Transfectants were treated with  $10^3$  IU/ml IFN- $\gamma$  for 16 h or IFN- $\alpha$  for 12 h. Luciferase assays were then carried out with the Dual-Glo luciferase assay system (Promega). Experiments were performed in triplicate and the data are expressed in relative luciferase units (RLU).

#### *Electrophoretic mobility shift assay (EMSA)*

EMSA was carried out as previously described (18). WT and/or mutant STAT1 plasmids were introduced into U3C cells by lipofection, with analysis 36 h after transfection. U3C transfectants or EBV-B cells were stimulated with  $10^5$  IU/ml IFNs for 20 minutes and a nuclear extract was then prepared as previously described.(18) We incubated 20  $\mu$ g (10  $\mu$ g for analyses of EBV-B cells) of nuclear extract with  $^{32}$ P-labeled ( $\alpha$ -dATP)

GAS (generated under control of the *FCGR1* promoter) or ISRE (*ISG15* promoter) probe for 30 minutes.

#### *Quantitative reverse transcription-PCR*

EBV-B cells were stimulated with  $10^3$  IU/ml of IFNs for 2 or 6 hours. Total RNA was then extracted with an RNeasy Mini Kit (QIAGEN, Germany). The cDNA was synthesized directly with random primers, by reverse transcription. *IRF1*, *CXCL9* and *ISG15* mRNA levels were determined by quantitative PCR (qPCR) on the cDNA, with the CFX96 Touch Real-Time PCR Detection System (Bio Rad, USA) and Taqman probes (Applied Biosystems). The results were normalized with respect to the values obtained for the endogenous *GAPDH* cDNA.

CD14-positive monocytes were purified from PBMCs by magnetic sorting (BD Biosciences, USA) and stimulated with  $10^3$  IU/ml IFN- $\gamma$  for 2 or 6 hours. The stimulated cells were then subjected to qPCR analysis, for the detection of *IRF1* and *CXCL9* mRNA.

#### *Cytokine determinations*

CD14-positive monocytes were used to seed 96-well plates ( $1.0 \times 10^5$ /well). They were

added to RPMI 1640 containing 10% FBS and cultured for 48 hours in the presence of 100 ng/ml LPS and various concentrations of IFN- $\gamma$  (10, 100 and 1000 IU/ml). TNF- $\alpha$  concentration in the supernatant was determined in duplicate, with a human TNF- $\alpha$  antibody bead kit (Invitrogen) and the Luminex 100 system (Luminex, USA).

#### *Flow cytometry*

PBMCs were stimulated with  $10^4$  IU/ml IFN- $\gamma$  for 15 minutes in the presence of FITC-conjugated anti-CD14 antibody (BD Biosciences). The cells were fixed by incubation with 200  $\mu$ l BD Cytofix buffer (BD Biosciences) for 10 min at 37°C, permeabilized by incubation with 400  $\mu$ l BD Phosflow Perm Buffer III (BD Biosciences) on ice for at least 30 min, and then stained with PE-conjugated anti-Stat1 antibody (pY701) (BD Biosciences). The cells were analyzed on a FACS Calibur apparatus (Becton Dickinson, USA).

#### Statistical analysis

Data are expressed as mean  $\pm$  Standard Deviation (SD). Statistical significance was calculated using analysis of variance followed by Tukey's post hoc analysis and SPSS software.  $P < 0.05$  was considered statistically significant.

**Supplementary Table S1** Laboratory data (Specific antibody) of the patients

Specific antibody	P1	P2	Negative range
Mumps IgG (EIA)	25.1	7.5	<2.0
Measles IgG (EIA)	<2.0	17.9	<2.0
Rubella IgG (EIA)	<2.0	34.3	<2.0
VZV IgG (EIA)	63.2	18.8	<2.0
Adeno (CF)	<4	<4	<4
Influenza (CF)	128	<4	<4
RSV (CF)	<4	<4	<4
EB VCA IgG (FA)	<10	80	<10
EBNA (FA)	<10	40	<10

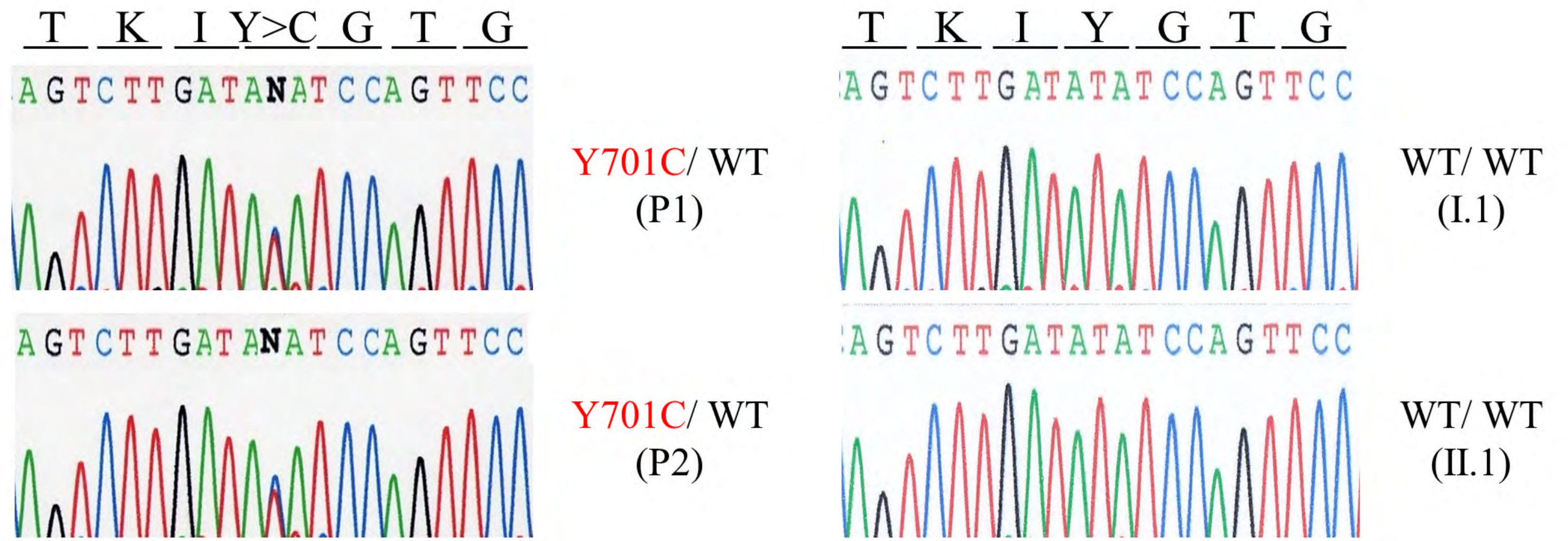
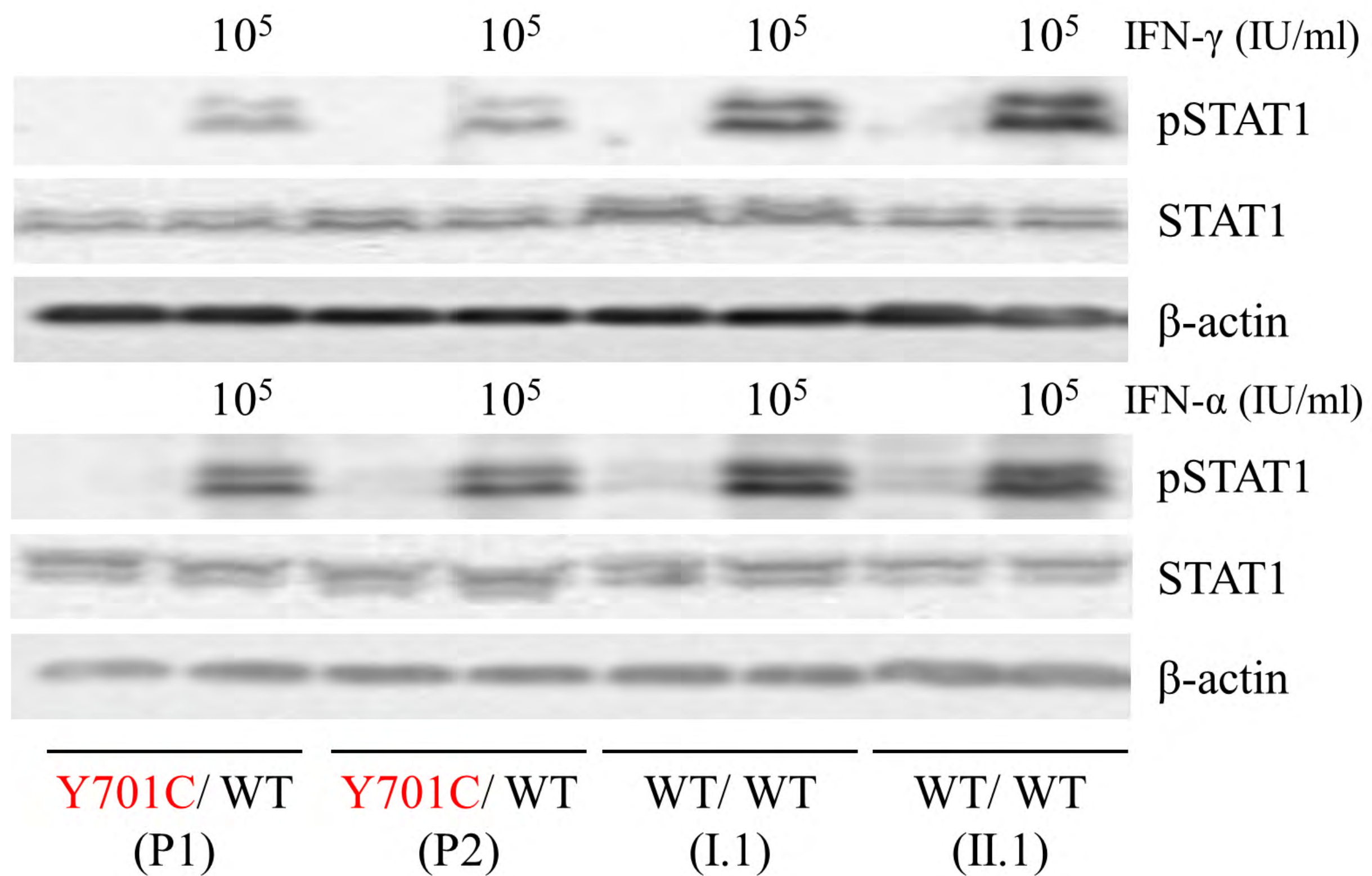
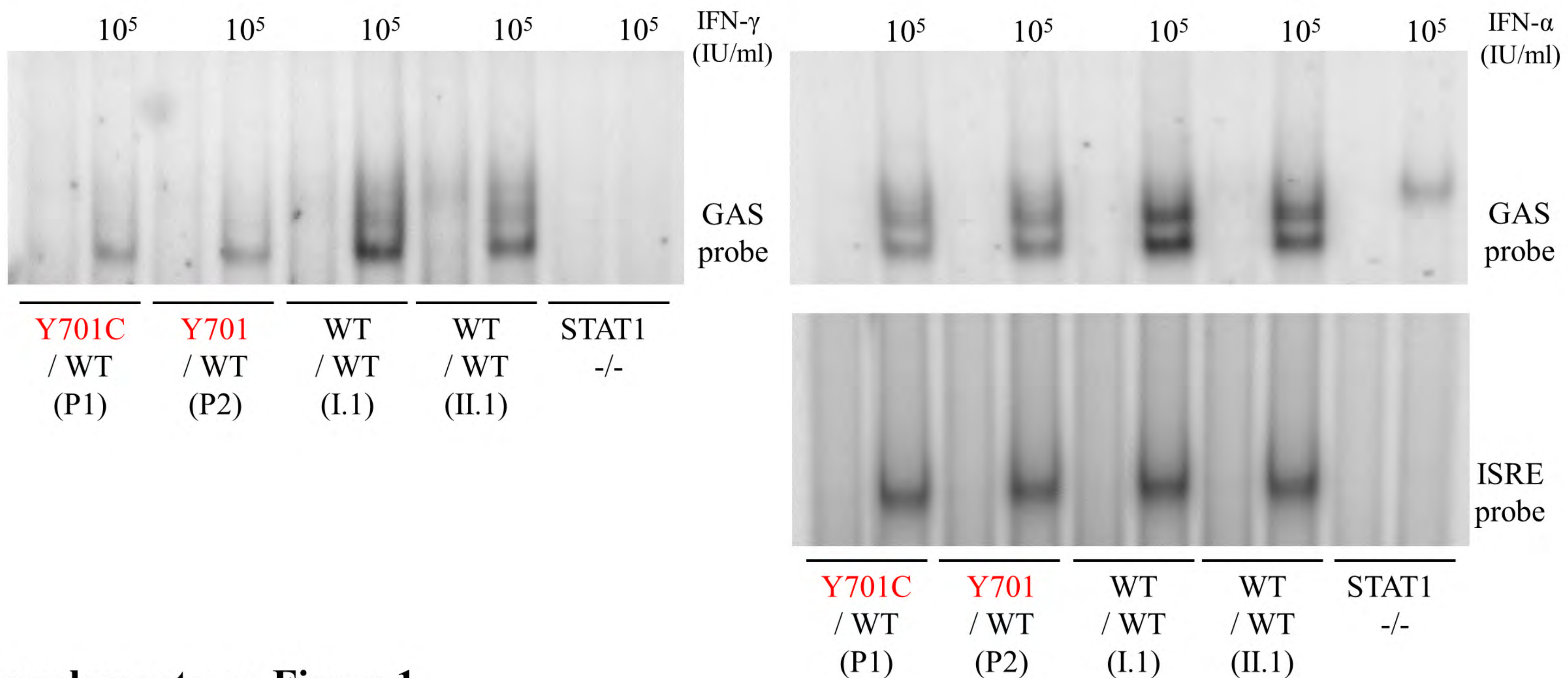
**Supplementary Table S2**

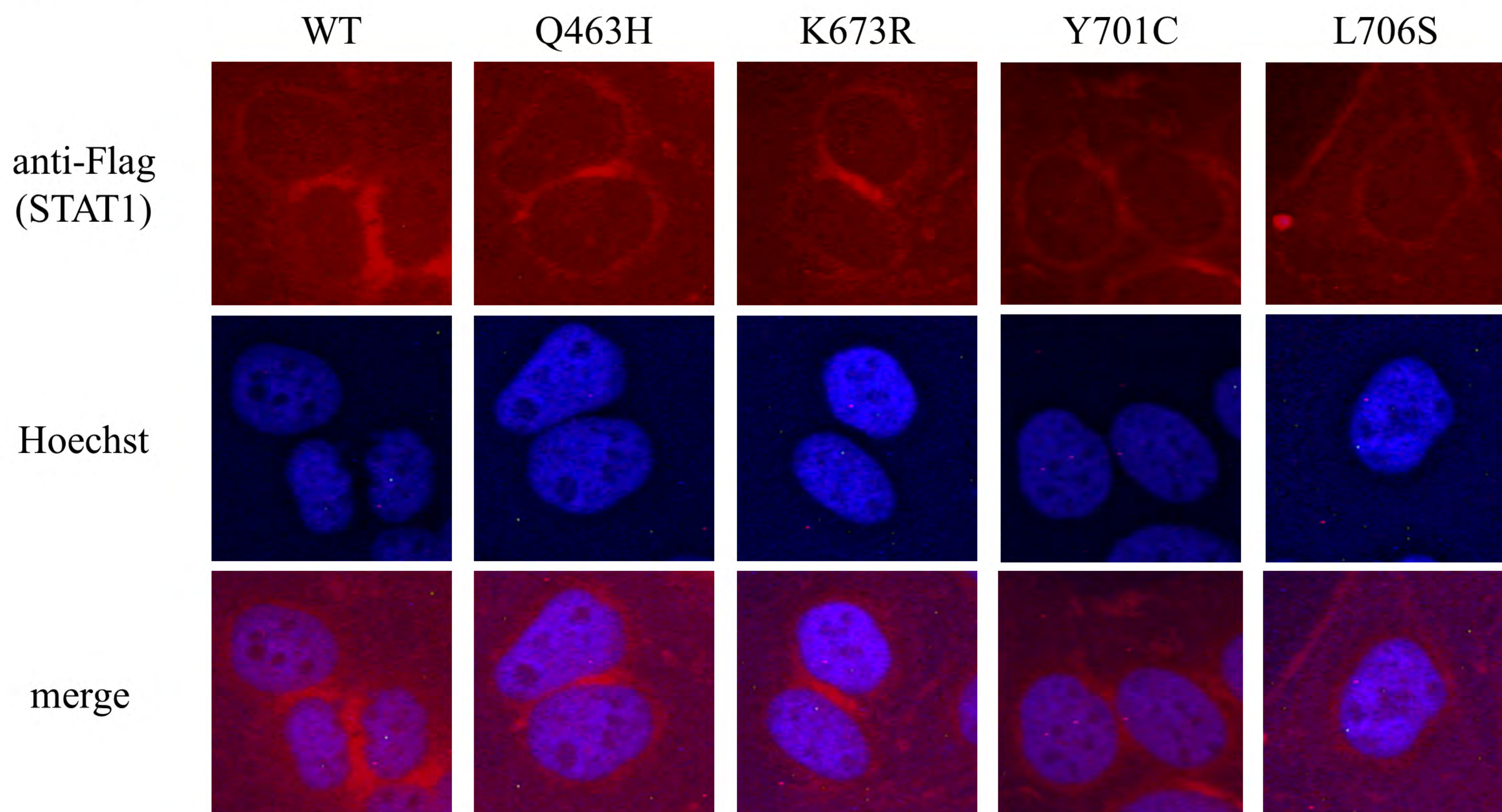
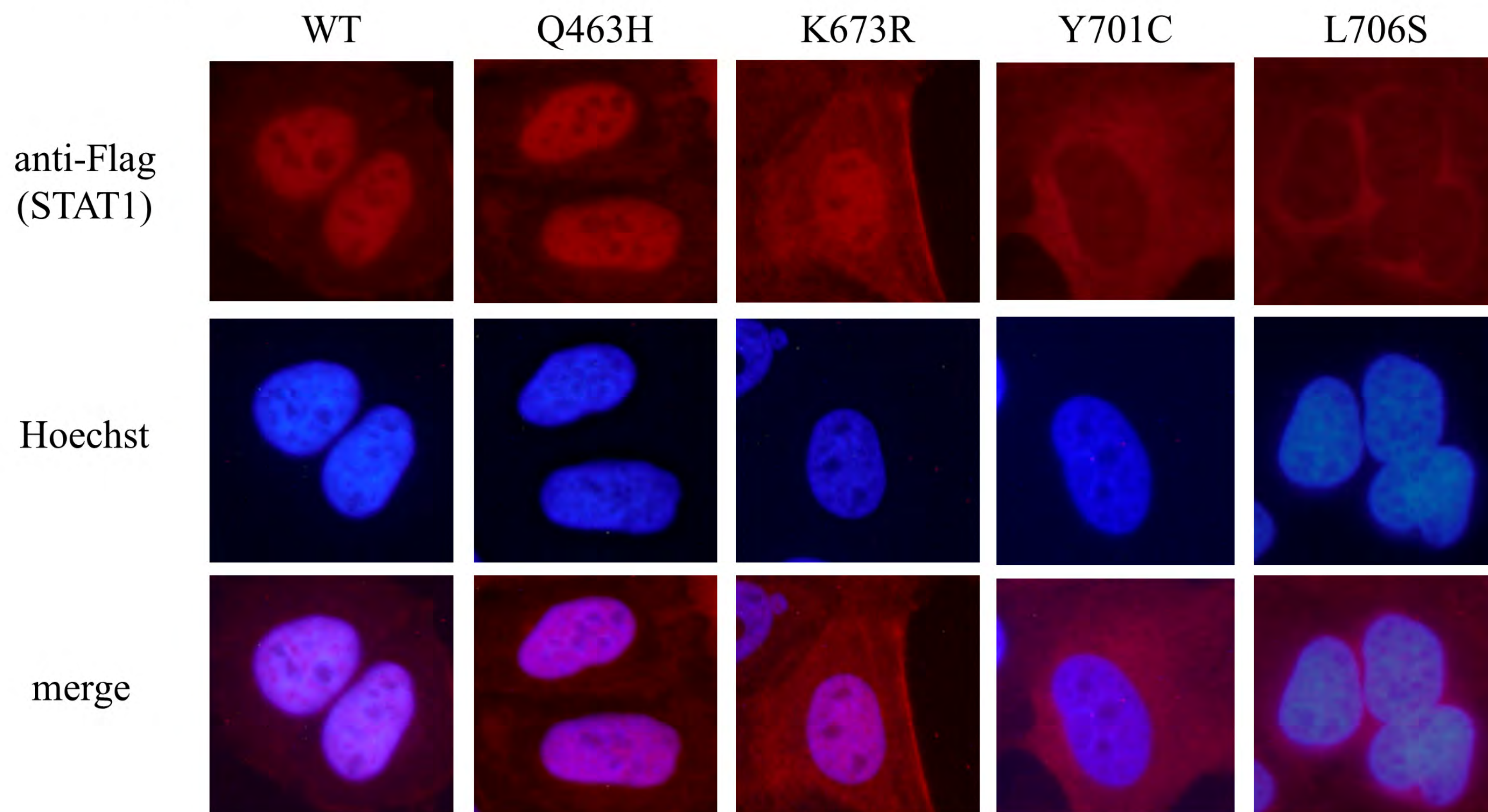
<b>Antibody</b>	<b>Species</b>	<b>Vendor</b>
Phosphorylated STAT1 (pY701)	rabbit	BD Bioscience
	rabbit	Cell Signaling
STAT1	rabbit	Cell Signaling
FLAG	mouse	Sigma-Aldrich
$\beta$ -actin	mouse	Sigma-Aldrich
Lamin A/C	mouse	Cell Signaling
GAPDH	mouse	Sigma-Aldrich



**Figure S1A**

Reverse

**Figure S1B****Figure S1C**

**Figure S2A**Before IFN- $\gamma$  stimulation**Figure S2B**After IFN- $\gamma$  stimulation

## Supplementary Figure Legends

### Figure S1.

(A) A heterozygous 2102 T>C (Y701C) mutation was detected in the patient (II.2) and his mother (I.2). (B) EBV-B cells from the patient (P1), his mother (P2) carrying Y701C mutation and other family members (I.1, II.1) were stimulated with  $10^5$  IU/ml IFNs for 15 min and subjected to immunoblotting. Cells from the patients (P1, P2) displayed an impairment of STAT-1 phosphorylation that was particularly marked following stimulation with IFN- $\gamma$ . (C) EBV-B cells from the patient (P1), his mother (P2) carrying the Y701C mutation and other family members (I.1, II.1) were subjected to EMSA with GAS and ISRE probes. Cells from the patients (P1, P2) displayed an impairment of GAF binding to DNA in response not only to IFN- $\gamma$ , but also in response to IFN- $\alpha$ . ISGF3-DNA binding levels upon IFN- $\alpha$  stimulation were almost normal in the patients' cells. At least two independent experiments were performed.

### Figure S2. Immunostaining of WT and mutant STAT1-producing cells

U2OS cells stably expressing Flag-tagged WT, Q463H, K673R Y701C, or L706S STAT1 were incubated without (A) or with (B) IFN- $\gamma$  for 30 min and stained with

FITC-tagged anti-Flag antibody for STAT1 protein and Hoechst 33342 (DAPI) for nuclei. (A) WT and mutant STAT1 proteins were present mostly in the cytoplasm before IFN- $\gamma$  stimulation. (B) After IFN- $\gamma$  stimulation, the WT and Q463H STAT1 proteins were found mostly in the nucleus. Nuclear translocation was severely impaired in cells producing the Y701C and L706S STAT1 proteins. The K673R STAT1 mutant was observed in both the nucleus and cytoplasm, suggesting incomplete nuclear translocation. Two independent experiments were carried out.